Studies on the Effect of Li_2SO_4 on the Structure of Lithium Borate Glasses

Munia Ganguli and K. J. Rao*

Solid State and Structural Chemistry Unit, Indian Institute of Science, Bangalore - 560 012, India

Received: July 9, 1998; In Final Form: November 2, 1998

Thermal and spectroscopic investigations have been carried out on a number of glasses with a wide range of compositions in the pseudoternary glass system, $Li_2SO_4-Li_2O-B_2O_3$, to understand the role of sulfate ions in modifying the borate glass structure. Both nuclear magnetic resonance (NMR) and infrared (IR) spectroscopic results indicate that four-coordinate boron atoms are retained in the glass structure to a greater extent in sulfate-containing glasses than in pure lithium borate glasses. There seems to be some evidence for the existence of sulfoborate-type units in Raman spectra in the region of 800−960 cm^{-1}. These conclusions are supported by the observed behavior of glass transition temperatures and molar volumes. The possibility of formation of sulfoborate-type units is discussed from bonding and thermodynamic points of view.

1. Introduction

Lithium ion conducting glasses have attracted the attention of solid-state scientists because of their possible application in lithium batteries.[1−6] Addition of suitable "dopant" lithium salts to glasses already modified by lithia has been found to lead to high lithium ion conductivities. Doping with lithium salts is often associated with interesting structural effects. It is therefore of vital importance to understand the structural aspects and their relation to lithium ion transport in them. In particular, it has been observed that lithium borate glasses doped with LiX (X = halogen) or Li_2SO_4 exhibit high conductivities.[7−10] The addition of lithium halides does not seem to result in any significant alteration of the network structure of the borate glass, and they appear to be simply dissolved in the glass matrix.[8,9] However, the role of added Li_2SO_4 in such glass matrixes seems to be more complex and not yet clearly understood. There have been several notable efforts made in this direction.[10−17]

The early Raman spectroscopic studies of Levasseur et al.[10] revealed the absence of any feature that could be associated with sulfate-borate interactions. Detailed IR and Raman spectroscopic studies by Kamitsos et al.[11] in the ultraborate and metaborate compositions also confirmed the absence of conclusive spectroscopic evidence for any structural effects. However, the authors noted that an increase of Li_2SO_4 in the glass composition is associated with an increase of the BO_4 tetrahedra as indicated by Raman vibrations (780 cm^{-1}) of modified boroxol rings containing one BO_4 tetrahedron; there was a direct increase of the intensities of the 780 cm^{-1} Raman peak with an increase in Li_2 SO_4. This was confirmed by the IR spectra (in the 850−1100 cm^{-1} range) in which there were corresponding intensity variations. Lithium ion conductivities and glass transition temperatures of lithium suphate doped borate glasses with compositions close to those of the metaborates were examined by Gandhi et al.,[12] who concluded that the high conductivity of these glasses was due to the participation of Li^+ ions from the dopant salt. It was suggested that Li_2SO_4 helps formation of more polar groups. However, Mustarelli et al.[13] carried out ^{11}B MAS NMR (magic-angle spinning nuclear magnetic resonance) studies at a field of 8.5 T and noted significant interaction of sulfate ions with the borate matrix. The authors interpreted this as being due to incorporation of SO_4^{2-} ions into the network, which therefore converts trigonal borons to tetrahedral borons. A mechanism was proposed suggesting that every SO_4^{2-} ion converts up to four or more BO_3 (B_3) units to BO_4 (B_4) units. More recently, Chryssikos et al.[14] have reexamined the IR and Raman spectra of Li_2SO_4-doped borate glasses. It is observed that Li_2SO_4 remains as a simply dissolved entity but influences the trigonal to tetrahedral boron conversion in a complex manner. An increased number of sulfate ions was found to slow the conversion of tetrahedral to trigonal borons. The spectra do not seem to provide any evidence for the formation of B−O−S bonds, which are required to be present if SO_4^{2-} ions were to be incorporated in the network. The results also suggest that at high Li_2SO_4 concentration there is a tendency toward formation of Li_2SO_4 microdomains. However, it may be noted that the IR spectra have been collected in the specular reflection mode, which often fails to reveal bulk features, and in fact, comparison of the IR spectra in refs 11 and 14 reveals significant differences such as shifts and absences of the vibrational peaks in the spectra collected by the specular reflection mode.

$Li_2SO_4-Li_2O-B_2O_3$ is an important glass-forming system and has already found application as a good lithium ion conducting electrolyte,[18,19] although several issues regarding its structure remain unresolved. Some of the issues are as follows. (a) Do the SO_4^{2-} ions get incorporated into the borate network? (b) Do NMR and IR spectroscopies provide a consistent picture of the effect of Li_2SO_4 on the three- and four-coordinate boron concentrations? (c) Since SO_4^{2-} is a doubly charged negative ion like O^{2-}, does it lead to similar structural consequences by behaving like a modifier? (d) If Li_2SO_4 is to behave simply as a solute in the borate glass matrix, would it induce structural modification purely as a consequence of geometrical packing restrictions?

To address these questions, it is required to investigate glasses over a wide range of compositions in this pseudoternary ($Li_2SO_4-Li_2O-B_2O_3$) system. Since B_4 concentration in borate glasses is known to increase at initial stages of modification and reach a maximum in the diborate composition (Li_2O-

* Correxponding author. Phone: +91-80-3092583. Fax: +91-80-3341683. E-mail: kjrao@sscu.iisc.ernet.in.

10.1021/jp982930z CCC: $18.00
Published on Web 01/22/1999

TABLE 1: Nominal Compositions of the Glasses Prepared in the $Li_2SO_4-Li_2O-B_2O_3$ Glass System, along with Their Codes

code	composition (mole fraction) Li_2SO_4	Li_20	B_2O_3
	CLSB Series		
CLSB1	0.3	0.35	0.35
CLSB2	0.3	0.39	0.31
CLSB3	0.3	0.42	0.28
CLSB4	0.3	0.45	0.25
CLSB	0.3	0.47	0.23
	CLOB Series		
CLOB1	0.1	0.5	0.4
CLOB2	0.15	0.5	0.35
CLOB3	0.2	0.5	0.3
CLOB4	0.25	0.5	0.25
	CB Series		
CB1	0.1	0.6	0.3
CB2	0.2	0.5	0.3
CB3	0.3	0.4	0.3
CB4	0.4	0.3	0.3
	CLB Series		
CLB1	0.0	0.5	0.5
CLB2	0.1	0.45	0.45
CLB3	0.2	0.4	0.4
CLB4	0.3	0.35	0.35
CLB5	0.4	0.3	0.3

$2B_2O_3$), the effect, if any, of Li_2SO_4 is not expected to be as remarkable and as sharply expressed when Li_2O/B_2O_3 is less than 1/2 as when Li_2O/B_2O_3 is greater than 1/2 in these glasses. Therefore, glass compositions in this work have been chosen to be such that Li_2O/B_2O_3 is greater than 1/2. It is also necessary to supplement spectroscopic data with other properties sensitive to structure and bonding such as molar volumes and glass transition temperatures, particularly in view of the questions raised above. In this paper, a number of glasses having such widespread compositions have been investigated using thermal and other characterization techniques besides IR, Raman, and ^{11}B MAS NMR spectroscopies. The results are discussed in the following sections keeping in view the questions raised above.

2. Experimental Section

Glasses were prepared by the conventional melt quenching method. The starting materials $Li_2SO_4 \cdot H_2O$ (BDH), Li_2CO_3 (Qualigens), and H_3BO_3 (BDH) (all of Analar grade) were taken in appropriate proportions and ground together to constitute a 5−10 g batch. The ground mixtures were heated in alumina crucibles at ~650 K for about 4−5 h in a muffle furnace. The temperatures were then raised to 1225 K when the charges were found to melt completely. They were held at 1225 K for about 10 min and stirred to ensure homogeneity. Then, they were quenched between stainless steel plates kept at room temperature. The nominal compositions of the glasses prepared, along with their codes, are listed in Table 1. Since the melts were held in the crucibles for about 10 min, it was assumed that no significant dissolution of alumina in the melt could have occurred. There was also no weight loss of the crucible (weight uncertainty being ~±0.002%), indicating that Al_2O_3 has not dissolved in the melt. However, no chemical analysis of the glass samples was performed, and only the nominal compositions are quoted throughout the text. These glasses have been grouped into four categories, and in each category, the proportion of one or a combination of two components is held constant. For example, in the CLOB series the percentage of Li_2O is held constant whereas in the CLB series Li_2O/B_2O_3 (lithium borate) is held constant. For the purpose of completion of the groups, four of the compositions find duplicate entries in two different categories in Table 1. The ternary compositional diagram for this glass system has been shown by Chryssikos et al.[14] The glasses were all transparent and colorless. Since they were slightly hygroscopic, the glass wafers were stored in desiccators over anhydrous $CaCl_2$ and taken out only at the time of measurement of their properties.

The amorphous nature of the samples was confirmed using powder X-ray diffraction (JEOL JOX-8P X-ray diffractometer). The glass transition temperatures (T_g) and heat capacities (C_p) were determined using a differential scanning calorimeter (Perkin-Elmer DSC 2). Dry nitrogen was used as a purge gas. For specific heat measurements, glass wafers weighing about 20−30 mg were taken in gold pans. The samples were first annealed at temperatures about 20 K below T_g (a rough estimate of T_g itself was obtained from a prior 20 K/min thermal scan), and DSC scans for C_p measurements were carried out at a uniform heating rate of 10 K/min. Single crystalline alumina (sapphire) was used as the calibration standard for calculating C_p. Accurate T_g values were determined as the intersection of the extrapolated linear portions around the glass transition region in the C_p vs T plots.

Densities (ρ) of annealed glass bits free of air bubbles and cracks (determined by visual examination) were measured by the standard Archimedian (apparent weight loss) method using xylene. The weights of the glass bits used were about 0.3−1 gm. The molar volume of each composition was calculated as $V_m = M/\rho$, where M is the molecular (formula) weight of the glass.

IR transmission measurements were made on pellets of the ground glass samples mixed with KBr in the range 4000−400 cm^{-1} using a Nicolet 740 FTIR spectrometer. Unpolarized Raman spectra were recorded (in the range 100−1500 cm^{-1}) on a SPEX 1403 Raman spectrometer making use of the excitation wavelength of 514.5 nm from an argon ion laser. Glass pieces of approximately 1 cm^2 area and 0.8−1 mm thickness were used for the Raman measurements.

^{11}B HRMAS NMR spectra of powdered glass samples were recorded using a Bruker DXL 300 solid-state high-resolution spectrometer (magnetic field = 7.05 T) operating at 96.4 MHz. Pulses of 5 μs duration at 90° were employed with a delay of 10 s between the pulses. A cylindrical zirconia rotor was used to spin the samples at speeds of 3−7 kHz. The spinning sidebands were identified by virtue of their drifts when samples were spun at different speeds. The chemical shift values were measured with respect to $(CH_3)_3B$.

3. Results and Discussion

3.1. Characterization Studies. *Molar Volumes*. The densities and molar volumes of all the glasses examined are listed in Table 2. The weighted sum of the molar volumes of the components of the glass in their crystalline state, V_c ($=xV_c(Li_2SO_4) + yV_c(Li_2O) + zV_c(B_2O_3)$, where x, y, and z are the mole fractions of Li_2SO_4, Li_2O, and B_2O_3, respectively) have also been listed alongside. Introduction of Li_2SO_4, while keeping the ratio of Li_2O/B_2O_3 in the glasses constant (CLB series) results in a considerable increase in the molar volume. In this series, the glass molar volumes are generally comparable to V_c values, although slightly higher, indicating that these glasses have a relatively more open structure. But in the other three series of glasses, molar volumes are somewhat lower than the V_c values. However, increasing Li_2SO_4 is always associated with increasing molar volume, irrespective of the Li_2O/B_2O_3 ratio

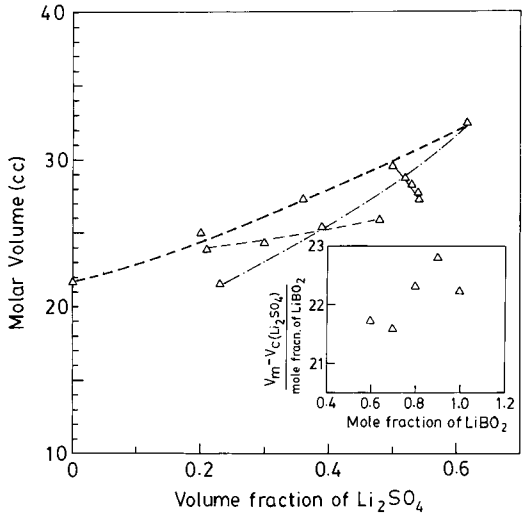

Figure 1. Variation of molar volume of all the glasses with volume fraction of Li_2SO_4 in $Li_2SO_4-Li_2O-B_2O_3$ glasses. Lines are drawn as guides to the eye: (—) CLSB series; (– - –) CLOB series; (–·–) CB series; (- - -) CLB series. (Inset: variation of molar volume of sulfate-free $LiBO_2$ in the CLB series with volume of $LiBO_2$.)

TABLE 2: Densities and Molar Volumes of All the Compostions in the $Li_2SO_4-Li_2O-B_2O_3$ Glass System

code	density, ρ (g/cm^3)	molar volume, V_m (cm^3)	total crystalline molar volume of the glass components, V_c (cm^3)	corrected RCP volume, V_{rcp} (cm^3)
		CLSB Series		
CLSB1	2.29	29.61	29.95	32.64
CLSB2	2.30	28.79	29.42	31.67
CLSB3	2.30	28.27	29.01	30.89
CLSB4	2.31	27.63	28.66	30.13
CLSB5	2.31	27.29	28.38	29.63
		CLOB Series		
CLOB1	2.25	23.90	23.69	26.37
CLOB2	2.29	24.37	24.75	26.99
CLOB3	2.27	25.47	25.81	27.62
CLOB4	2.31	25.90	26.87	28.26
		CB Series		
CB1	2.31	21.56	22.34	23.85
CB2	2.27	25.47	25.81	27.62
CB3	2.29	28.74	29.28	31.39
CB4	2.27	32.53	32.74	35.15
		CLB Series		
CLB1	2.29	21.72	21.57	25.11
CLB2	2.23	25.01	24.36	27.62
CLB3	2.26	27.34	27.16	30.14
CLB4	2.29	29.61	29.95	31.78
CLB5	2.27	32.53	32.74	35.15

as seen in the CB and CLOB series. When Li_2SO_4 is held constant (CLSB series) and the Li_2O/B_2O_3 ratio is increased, there is only a slight decrease in the molar volume. Thus, in Figure 1, the variation of the molar volume V_m of the glass and the calculated volume fraction of $Li_2SO_4(xV_c(Li_2SO_4)/V_m)$ seems to exhibit a good positive correlation for all the glasses. To examine the effect of Li_2SO_4 on glass molar volumes, particularly in view of the suggestions that Li_2SO_4 is simply dissolved in the borate glass matrix, the actual volume of Li_2SO_4 has been subtracted from the molar volumes of the glasses and the effective molar volume of the Li_2SO_4-free borate glass itself has been evaluated in the case of the CLB series. It is plotted as an inset to Figure 1. It is seen that, compared to the molar volume of pure lithium metaborate glass itself, the effective molar volumes of Li_2SO_4-doped glasses exhibit a nonuniform variation. A maximum of about 2.6% deviation is observed, which is much higher than the uncertainties in molar volume measurements. Although it is assumed that the molar volume of Li_2SO_4 in the glass is the same as that of crystalline Li_2SO_4, it would make no difference either to the nature of the variation or its magnitude even if it were slightly different. The figure inset also suggests that the effective molar volume increases by incorporation of Li_2SO_4 out to ~10 mol %, above which it decreases out to ~40 mol % Li_2SO_4. This suggests that Li_2SO_4incorporation may not be a simple dissolution process.

In the glass compositions chosen for this investigation, the Li_2O/B_2O_3 ratio is greater than 1/2 and only metaborate, pyroborate, or orthoborate species are expected to be present in the glass. Thus, B_3 units are expected to be in higher concentration than B_4. The presence of trigonal borons, with one or two nonbridging oxygens in them, particularly when they are a part of extended chains, diminishes the scope for folding of chains and formation of densely packed structures by strong interchain Coulombic repulsions. This aspect has been examined by calculating the random close packed (RCP) volumes of oxide ions assuming that borons are embedded at the centers of three oxygen atoms or in the tetrahedral voids while Li^+ ions are placed only in the tetrahedral voids. Tetrahedral voids occupied by Li^+ ions expand due to the larger size of Li^+ ions compared to the void size (void size can be at most 0.22 Å × 1.36 Å = 0.3 Å, where 1.36 Å is the radius of the oxygen ion, while the radius of the Li^+ ion is 0.68 Å). These void expansions are followed by positional readjustments of other oxide ions, which thereby localize as much as possible the effect of expansion and try to share the increased volume. The increased volume can be calculated on a "per oxide ion" basis, and the correction to the RCP volume is calculated by multiplying this by the total number of oxide ions present in the system. For example, in CLB1, the RCP volume corrected for the insertion of the lithium ions can be calculated in the following way:

RCP volume of only the $2N$ oxide ions present in 1 mol of CLB1 (oxide ion radius of 1.36 Å) would be

$$((2N(4\pi/3)(1.36)^3) \times 10^{-24})/0.63 = 20.14 \text{ cm}^3$$

where N is the Avogadro number and 0.63 is the packing fraction of the RCP assembly. Li^+ and B^{3+} ions may be considered as simply embedded in the voids of the RCP assembly of O^{2-} ions. B^{3+} takes positions at triple junctions, and the cavity radius of 0.21 Å of such junctions is adequate for B^{3+} ion occupation. The tetrahedral borons find the radius of tetrahedral voids adequate for them. Since RCP results in the formation of tetrahedral voids almost exclusively,[20,21] the radius of the embedded ion can be at the most 0.3 Å (0.22 Å × 1.36 Å) and cannot therefore accommodate the Li^+ ion (of radius 0.68 Å). The tetrahedral cavity therefore expands, and the RCP volume also increases. The cavity radius increases by (0.68 − 0.3) Å, i.e., 0.38 Å, and in the process the four surrounding O^{2-} ions are assumed to move outward isotropically. To a first approximation, this expansion due to the insertion of Li^+ ions can be treated as a corrective volume of

$$((4\pi/3)(N/2)[(\sqrt{3}a/2 + 0.38)^3 - (\sqrt{3}a/2)^3]) \times 10^{-24} = 4.97 \text{ cm}^3$$

where $\sqrt{2}a$ is the interoxygen ion distance in the tetrahedron. Thus, the molar volume of the $LiBO_2$ glass should be (20.14 + 4.97) cm^3 = 25.11 cm^3. These estimated RCP volumes of the glasses are listed in Table 2. It may be seen that the calculated RCP volumes are uniformly higher than the actual molar

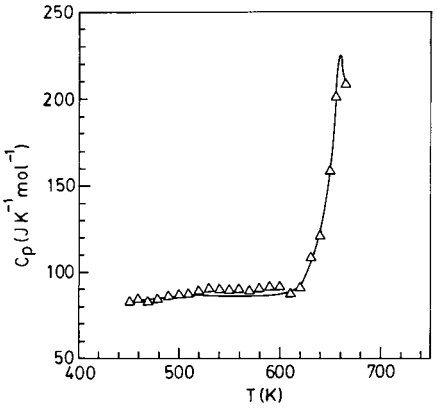

Figure 2. Variation of specific heat with temperature in a representative composition (CLOB1) of the $Li_2SO_4-Li_2O-B_2O_3$ glass system.

TABLE 3: Thermal Properties of the $Li_2SO_4-Li_2O-B_2O_3$ Glasses

sample	T_g (K)	C_p (at T_g − 20K) (J K^{-1} mol^{-1})	$3nR$ (J K^{-1} mol^{-1})
		CLSB Series	
CLSB1	610	120.1	122.2
CLSB2	592	119.8	120.2
CLSB3	590	115.2	118.7
CLSB4	575	107.2	117.5
CLSB5	560		116.5
		CLOB Series	
CLOB1	632	87.5	104.8
CLOB2	618	90.5	107.3
CLOB3	592	101.2	109.8
CLOB4	585	100.1	112.2
		CB Series	
CB1	620	78.5	99.8
CB2	592	101.2	109.8
CB3	585	107.8	119.7
CB4	570	120.4	129.7
		CLB Series	
CLB1	690	98.9	99.8
CLB2	670	103.4	107.3
CLB3	645	112.6	114.7
CLB4	610	120.1	122.2
CLB5	570	120.4	129.7

volumes, indicating that the packing in these glasses is significantly more efficient than that in a RCP arrangement. Since in the case of Li_2SO_4-free lithium metaborate glass itself this difference between RCP and actual volumes is clearly evident, a large part of this is quite likely to be due to the fact that the effective radius of the oxide ions present in borate must be lower than 1.36 Å (r_{B-O} in B_2O_3 is 1.39 Å[22] therefore $r_O{}^{2-}$ in B_2O_3 is only 1.19 Å). Since the difference between RCP and actual volumes of glasses is present to a greater extent in all Li_2SO_4-containing glasses, a part of this difference is perhaps attributable to the interaction between borate and sulfate units.

Thermal Properties. The glass transition temperatures (T_g) of the various glasses, the heat capacities at (T_g − 20) K, and the Dulong−Petit heat capacities are listed in Table 3. The observed glass transition behavior was invariably fairly sharp and steplike in all cases. There was also clear evidence of relaxational overshoots in heat capacity plots, as expected for these ionic glasses (see Figure 2). Because of the tendency of these glasses to crystallize just above T_g (above the region of the overshoot), reliable and reproducible values of ΔC_p could not be obtained. The T_g values show a wide spread of 560−690 K over the entire range of compositions. A close inspection of the variation of T_g with composition in the CLB series reveals that increasing Li_2SO_4 decreases the glass transition temperature

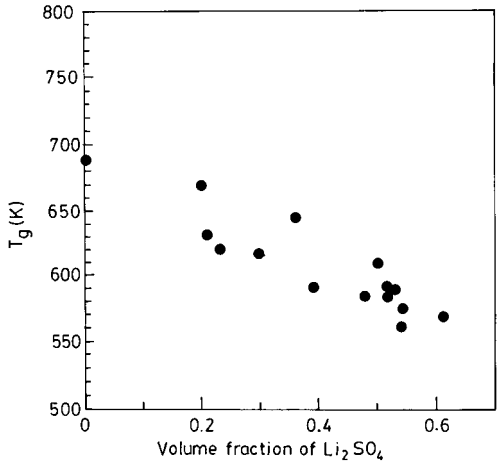

Figure 3. Glass transition temperatures as a function of the volume fraction of Li_2SO_4 in $Li_2SO_4-Li_2O-B_2O_3$ glasses.

strongly. Holding the Li_2SO_4 concentration constant and varying the molar proportions of Li_2O and B_2O_3 over a wide range does not seem to affect T_g as much as is evident from the T_g data for the CLSB series. Furthermore, in case of the CB and CLOB series T_g data, the ratio of Li_2O to B_2O_3 is varied in opposite directions but the trend of the variation of glass transition temperatures is the same and is inversely related to the concentration of Li_2SO_4. Therfore, the T_g is clearly influenced most by the Li_2SO_4 concentration, as evident from Figure 3. We will show later that T_g varies almost linearly as a function of the $SO_4{}^{2-}$ ion fraction of the total anion content of the glass. There is no manifestation of a separate glass transition feature to suggest that a Li_2SO_4-rich phase remains as a separate (and presumably glassy) phase (microdomains).

The heat capacities of all the glasses are lower than the corresponding Dulong−Petit heat capacities. The differences between Dulong−Petit and actual heat capacities appear to be greater in more modified (Li_2O/B_2O_3 being higher) glasses. Thus, in CLSB4, CLOB4, and CB1 glasses the differences are very high ($C_p/(3nR) = 0.91$ in CLSB4 and 0.79 in CB1). In the metaborate compositions in general, this difference is low (note the difference of only 0.9 J K^{-1} mol^{-1} in pure $LiBO_2$ glass CLB1). But this difference is high when Li_2SO_4concentration in the glasses increases as in CLB5. Therefore, the differences between the Dulong Petit and observed heat capacities appear to be high when both the Li_2SO_4concentration and Li_2O/B_2O_3 ratios are high. This again suggests the possibility that the various B_3 species interact with $SO_4{}^{2-}$ ions and suppress the number of available thermally excitable modes, which therefore increases the differences between the observed and Dulong−Petit heat capacities.

3.2. Spectroscopic Investigations. *Infrared Spectra.* Alkali-modified borate glasses are known to possess complex structural units that depend on the degree of alkali oxide fraction.[23−25] Infrared spectroscopy has been used in the mid-IR region to identify the nature of the anionic species present in these glasses, and the spectra are shown in Figure 4a−d. The only two modes of the $SO_4{}^{2-}$ ions which are infrared active are the ν_3 and ν_4, which are due to asymmetric stretching (1135 cm^{-1}) and bending (645 cm $^{-1}$), respectively.[11] These modes are present in all the glasses except in CLB1, in which $Li_2SO_4$is absent.

It has been observed that borate glasses show infrared bands in the region between 1150 and 1500 cm^{-1} due to B−O vibrations of B_3 units and in the 800−1150 cm^{-1} region due to vibrations of the B_4 units.[11,26−29] The bending vibrations are expected to be present around 730 cm^{-1}.[11,26−29] Examination

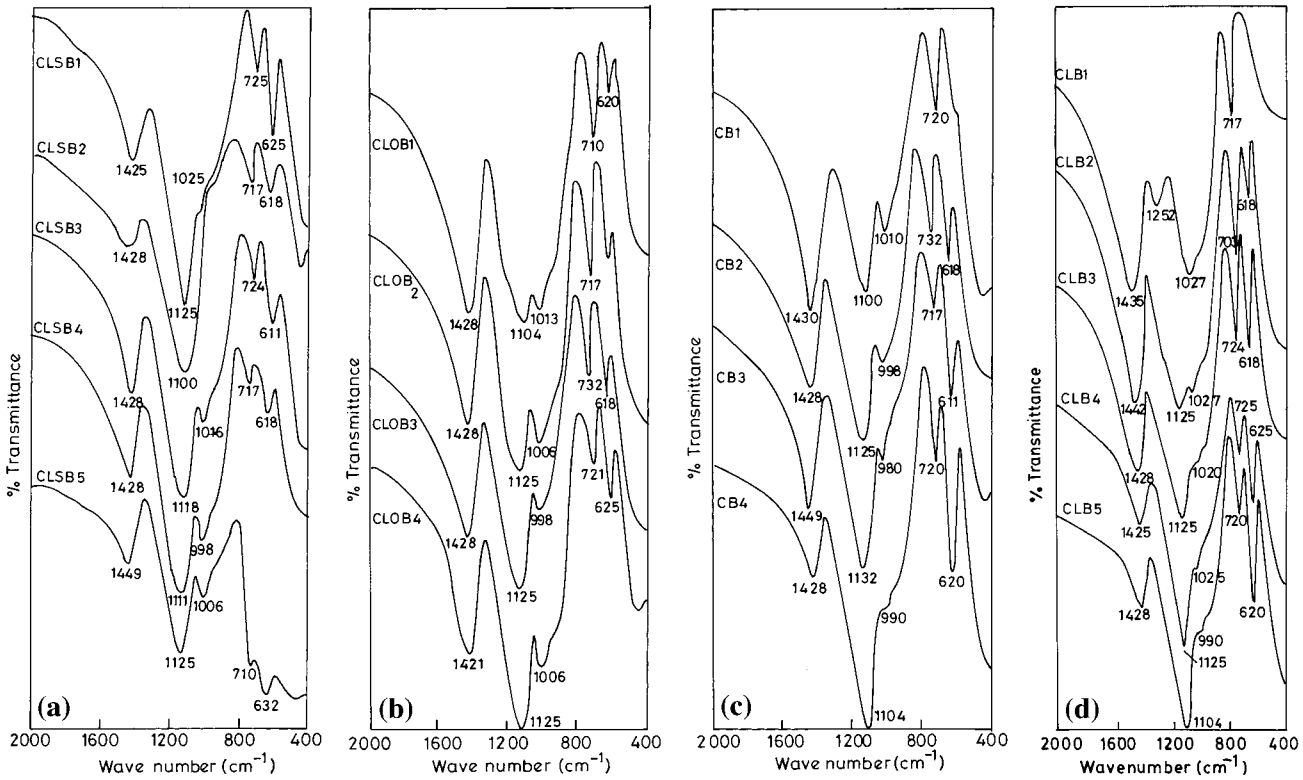

Figure 4. Infrared spectra of (a) constant Li_2SO_4 (CLSB) glass series, (b) constant Li_2O (CLOB) glass series, (c) constant B_2O_3 (CB) glass series, and (d) constant Li_2O/B_2O_3 (CLB) glass series in the glass system $Li_2SO_4-Li_2O-B_2O_3$.

of the spectra of the CLB series of glasses reveals that in CLB1 peaks due to both B_4 (1027 cm^{-1}) and B_3 (1250 and 1435 cm^{-1}) are present along with peaks due to B−O−B bending modes at 717 cm^{-1}. The addition of Li_2SO_4 results in development of new bands at around 1120 and 620 cm^{-1} that are due to vibrational frequencies of the sulfate group as mentioned earlier. There is clear evidence of a decrease in the intensity of the 1435 cm^{-1} peak down the series, whereas the weak peak at 1250 cm^{-1} disappears altogether. This is possible only if the number of B_3 units decreases as the Li_2SO_4 concentration in the glass increases. It is difficult to ascertain if B_3 is converted into B_4 units because of the lack of corresponding increase in intensity of the B_4 peak at ∼1027 cm^{-1}. The dominance of the strong peak at ∼1120 cm^{-1} due to SO_4^{2-} ions makes the 1027 cm^{-1} peak appear like a subdued shoulder.

In the CB series also, while it is clear that the concentration of B_3 decreases as manifested in the weakening of the intensity of the 1428 cm^{-1} peak, the corresponding change in the intensity of the 1027 cm^{-1} peak is not so evident to conclude that B_4 has increased. This is again due to the dominance of the 1100 cm^{-1} sulfate peak. There are no other significant changes in the IR spectra of glasses in the CLSB and CLOB series. Although absorptions due to B_3 and B_4 are identifiable in both, it is difficult to ascertain any structural changes by addition of $Li_2SO_4$to the glass by the use of only IR spectra.

However the 1435 and 1027 cm^{-1} peaks are characteristic of B_3 and B_4 units respectively in the glass structure, and it is still possible to examine the variation of their relative intensities in the IR spectra by considering their intensities as simply proportional to the amplitudes (although it would have been more appropriate to use areas under the peaks). This approximation was necessitated since it was both difficult to deconvolute the 1027 cm^{-1} peaks in Figure 4a−d and doubtful whether the procedure gave accurate results. It was found useful to calculate $N_4(\mathrm{IR}) = B_4/(B_3 + B_4)$ as the ratio $A_{1027\mathrm{cm}^{-1}}/(A_{1027\mathrm{cm}^{-1}} + A_{1435\mathrm{cm}^{-1}})$, where A refers to the amplitude of the IR peak. It will be shown later that the variation of N_4(IR) is very consistent with the variation of N_4 obtained from NMR data. N_4 values from both NMR and IR confirm the well-documented influence of lithium sulfate in retaining tetrahedral B_4 units in the glass.

Raman Spectra. Raman spectra of the glasses studied here are given in Figure 5a−d. Raman-active SO_4^{2-} vibrations are expected to appear in the regions of 465 (ν_2, bending), 645 (ν_4, bending), 1010 (ν_1, symmetric stretch), and 1135 cm^{-1} (ν_3, asymmetric stretch).[11] The 465, 645, and 1010 cm^{-1} peaks are very clearly in evidence in all the spectra except for the case of CLB1, in which $Li_2SO_4$is absent.

In the CLB series, pure lithium metaborate glass shows Raman peaks at 535 and 765 cm^{-1} that are generally attributed to B−O vibrations in isolated diborate groups and vibrations of boroxol rings in which one of the borons is four-coordinate, respectively. The 970 cm^{-1} scattering is due to B−O$^-$ stretching in smaller borate units, and the one at 1485 cm^{-1} is generally attributed to B−O$^-$ stretching in metaborate groups.[27,28,30−34] Addition of Li_2SO_4 not only gives rise to peaks due to SO_4^{2-} ions but also causes significant changes in the spectra arising from the borate network. Isolated diborate groups seem to be destroyed on addition of Li_2SO_4 since the peak at 535 cm^{-1} disappears, and new peaks develop in the region of 800−950 cm^{-1}. Spectral features in this region are known to arise from B−O$^-$ stretching in pyroborate or orthoborate groups.[27,28] Since the emergence of these features is due to addition of Li_2SO_4, and not due to increasing Li_2O content in the CLB series, they can be associated with some entirely new species produced by addition of Li_2SO_4, and this aspect is discussed in a later section. While it is not certain as to whether the 967 cm^{-1} peak disappears or gets merged into the 1010 cm^{-1} peak of sulfate vibrations, the peak at 1485 cm^{-1} clearly weakens on addition of Li_2SO_4, indicating reduction in the concentration of metaborate groups.

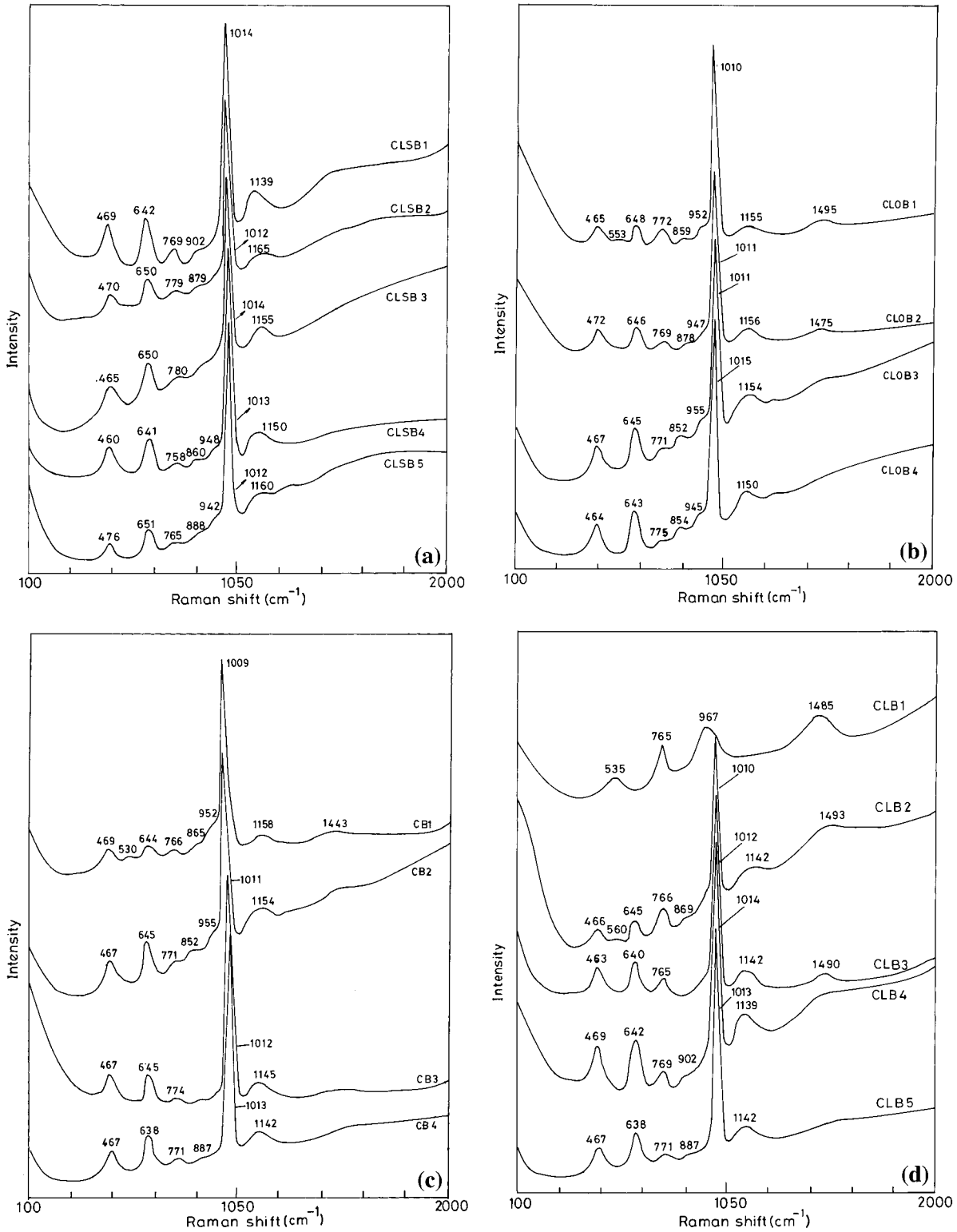

Figure 5. Raman spectra of (a) constant Li_2SO_4 (CLSB) glass series, (b) constant Li_2O (CLOB) glass series, (c) constant B_2O_3 (CB) glass series, and (d) constant Li_2O/B_2O_3 (CLB) glass series in the glass system $Li_2SO_4-Li_2O-B_2O_3$.

In the CLSB series, where the ratio of Li_2O to B_2O_3 is increased, keeping the proportion of Li_2SO_4 constant, emergence of peaks in the region of 860−950 cm^{-1} is most probably due to formation of smaller borate units such as pyroborates and orthoborates.[28,29] Such species are present in the CLOB series of glasses also and grow more prominent with increasing Li_2O/B_2O_3. The existence of B_4 units is confirmed by the peak at ∼770 cm^{-1}. Further, an increase of Li_2SO_4 in the glasses is associated with the disappearance of the broad peak at 1485 cm^{-1} associated with metaborate units. The spectra of the CB series of glasses also reveal the presence of B_4 and small charged borate units derived from B_3. The nature of the structural species expected to be present in all the glass compositions investigated here will be discussed in a later section.

^{11}B MAS NMR Spectra. ^{11}B MAS NMR spectra have been determined for all the samples (see Figure 6a−d), and they exhibit a sharp resonance at around −17 ppm (with respect to the resonance signal of trimethyl boron[35]) and arise from B_4

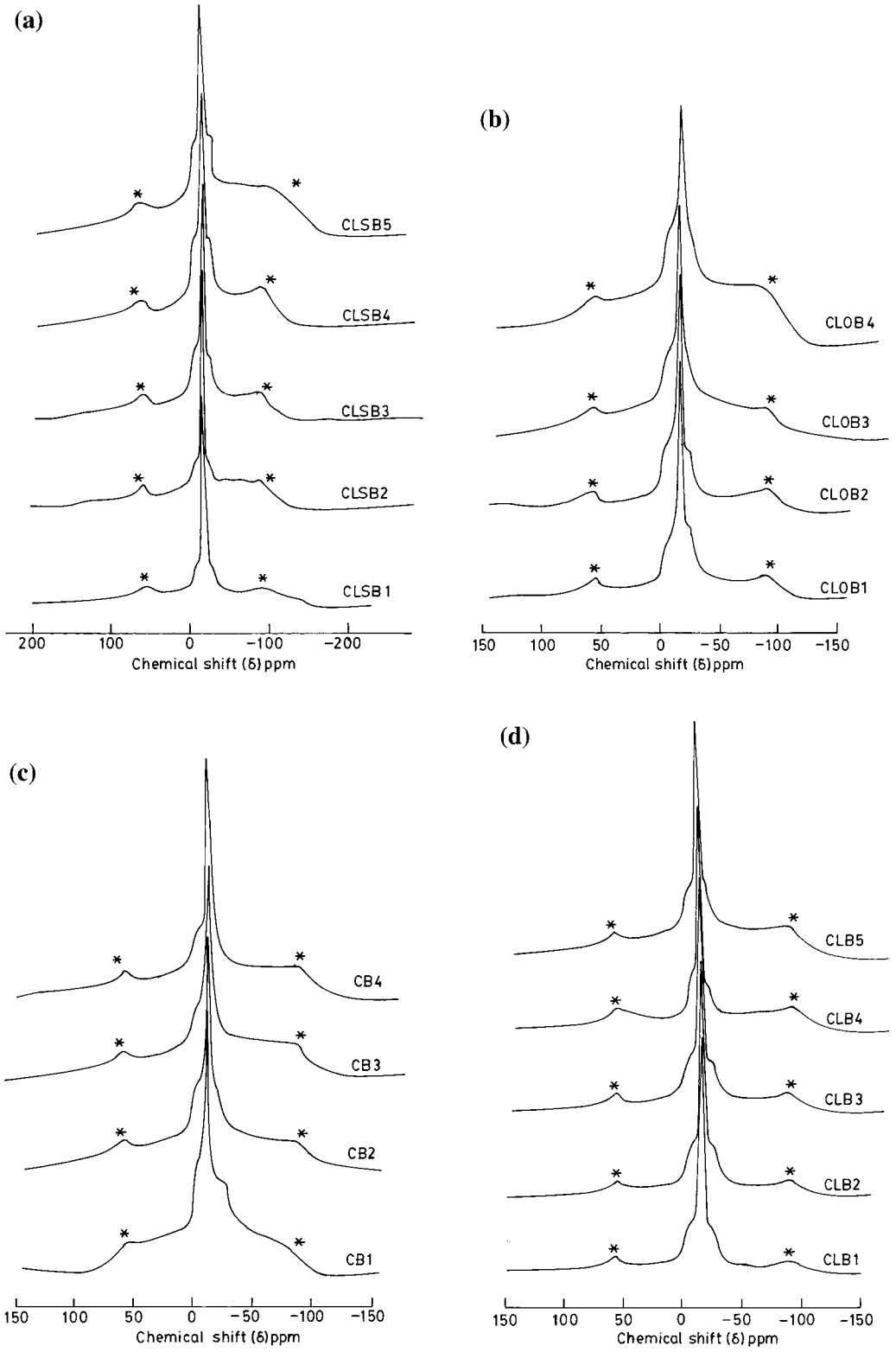

Figure 6. ^{11}B MAS NMR spectra of (a) constant Li_2SO_4 (CLSB) glass series, (b) constant Li_2O (CLOB) glass series, (c) constant B_2O_3 (CB) glass series, and (d) constant Li_2O/B_2O_3 (CLB) glass series in the glass system $Li_2SO_4-Li_2O-B_2O_3$. The spectra were recorded at a spinning speed of 7 kHz.

species. There is also a split peak at the base of all the signals from B_4, which arises from three-coordinate boron atoms, B_3.[36,37] Thus, all the spectra have the appearance of a B_4 resonance peak with wings at the base as is expected in glasses containing boron in dual coordination.[36−45] The area under the composite spectrum has been apportioned to B_4 and B_3 present in the glass by connecting the peaks of the quadrupolar split B_3 with a smooth line. Such apportionment is somewhat approximate,[36,37,41,45] but there appears to be only a small uncertainty in the proportions of B_4 and B_3 obtained in this manner. The trends in their variation can be considered to be very reliable as demonstrated earlier.[36,37] The values of $N_4(\mathrm{NMR}) = B_4/(B_3 + B_4)$ have been calculated for all the glasses and are listed in Table 4.

It is seen from Table 4 that in the CLSB series, where the concentration of Li_2SO_4 is held constant and the Li_2O/B_2O_3 ratio

TABLE 4: Relative Proportions of the Different Structural Species in Li_2SO_4−Li_2O−B_2O_3 Glasses as Determined from ^{11}B HRMAS-NMR and Chemical Composition

			different borate species expressed as mole fraction of B_2O_3				
sample	N_4 (NMR)	N_4 (IR)	Li_2SO_4	B_4	B_3^-	B_3^{2-}	B_3^{3-}
CLSB Series							
CLSB1	0.45	0.59	0.3	0.158	0.192		
CLSB2	0.41	0.5	0.3	0.128	0.106	0.078	
CLSB3	0.37	0.48	0.3	0.104	0.176	0.14	
CLSB4	0.27	0.46	0.3	0.069		0.181	0.005
CLSB5	0.28	0.44	0.3	0.065		0.1025	0.065
CLOB Series							
CLOB1	0.32	0.49	0.1	0.128	0.172	0.1	
CLOB2	0.36	0.5	0.15	0.126	0.074	0.15	0.014
CLOB3	0.38	0.52	0.2	0.114		0.172	
CLOB4	0.39	0.53	0.25	0.098		0.055	0.098
CB Series							
CB1	0.27	0.44	0.1	0.081		0.138	0.081
CB2	0.38	0.52	0.2	0.114		0.172	0.014
CB3	0.46	0.56	0.3	0.138	0.062	0.1	
CB4	0.49	0.64	0.4	0.147	0.153		
CLB Series							
CLB1	0.38	0.52	0.0	0.19	0.31		
CLB2	0.38	0.52	0.1	0.171	0.279		
CLB3	0.41	0.54	0.2	0.164	0.236		
CLB4	0.45	0.59	0.3	0.158	0.192		
CLB5	0.49	0.64	0.4	0.147	0.153		

is progressively increased, there is a decrease in the N_4 value. This is expected since increasing the ratio of Li_2O/B_2O_3 to values greater than 1/2 is known to result in reconversion of B_4 into smaller B_3 units.[45] In all the other three series, where Li_2SO_4-concentration is increased, N_4(NMR) is also found to increase. What is even more surprising is that while the trends in the variation of Li_2O/B_2O_3 are opposite in the CLOB and CB series, N_4 increases in both of them. Thus, the $B_4 = B_3$ equilibrium is influenced not just by the Li_2O/B_2O_3 ratio but by the presence of Li_2SO_4 also. In the CLOB and CB series in which the concentration of Li_2SO_4 is increased down the series, it seems that the conversion of B_4 to B_3 is hemmed in by Li_2SO_4. This is even more clearly evident in the CLB series where the concentration of Li_2SO_4 is increased while holding the Li_2O/B_2O_3 ratio constant and N_4 is found to increase.

Structural Implications. A well-established feature of borate glasses is that their modification by addition of ionic oxides first leads to conversion of B_3 to B_4 up to where the proportions of B_3 and B_4 are equal. Further addition of modifier oxide leads to a decrease of B_4 by conversion to charged B_3 units such as *meta*-($[BO_{2/2}O]^-$), *pyro*-($[BO_{1/2}O_2]^{2-}$), and *ortho*-($[BO_3]^{3-}$) borate units.[40] Formation of B_4 units is assumed to occur initially through the formation of oxygen bridges between $[BO_{3/2}]_n$ units in B_2O_3. Such bridging introduces a three-dimensional character to the structure, which however, begins to break down when the B_4/B_3 ratio exceeds unity. Thus, N_4 ($=B_4/(B_3 + B_4)$) is always less than 0.5 and has been confirmed by structural studies in a variety of alkali-modified borate glasses.[36,37,39,40]

N_4 is most sensitively determined by making use of ^{11}B HRMAS NMR. As pointed out earlier, B_4 and B_3 species give rise to overlapping resonance peaks, the area under which can be deconvoluted to obtain N_4 values.[36,37,39,45]

These three-coordinate boron atoms in the present glass system are distributed among different B_3^{n-} species with $n = 1-3$ (B_3^- is the metaborate, B_3^{2-} is the pyroborate, and B_3^{3-} is the orthoborate species). Since the quantity of modifying oxide (Li_2O) present in the system is also known, it is possible to determine all the B_3 species quantitatively by imposing the condition of charge neutrality and hierarchy of modification. By the latter it is meant that the charged B_3 species form and transform in the order B_3^-, B_3^{2-}, and B_3^{3-} as modifier concentration increases. The procedure of calculation of the various borate species is illustrated for the sample CB1 as follows.

The composition of 1 mol of CB1 from Table 1 is 0.1 mol of Li_2SO_4, 0.6 mol of Li_2O, and 0.3 mol of B_2O_3. The experimental value of N_4 given in Table 4 is 0.27, which means

$$B_4/(B_3 + B_4) = 0.27$$

$B_3 + B_4 = 2z$, where z is the mole fraction of B_2O_3 in the glass and is equal to $2 \times 0.3 = 0.6$ mol.

Hence, $B_4 = 0.27 \times 0.6 = 0.162$ mol. Thus, we have 0.438 mol of B_3 and 0.162 mol of B_4 in the glass. The formation of 0.162 mol of B_4 units present in glass would have used up 0.081 mol of Li_2O. Therefore, the remaining 0.519 mol, i.e., (0.6 − 0.081) mol of Li_2O, can be considered as having been utilized in the modification of 0.438 mol of B_3^0 into various charged B_3 units. An amount of 0.438 mol of B_3^0 would first use 0.219 mol of Li_2O to be converted to 0.438 mol of B_3^- according to the equation

$$2[BO_{3/2}]^0 + Li_2O = 2[BO_{2/2}O]^-$$

There is still an excess of (0.519 − 0.219) = 0.3 mol of Li_2O in the glass, and therefore, there is scope for B_3^- to be modified further to B_3^{2-}. Hence, 0.438 mol of B_3^- reacts further with 0.219 mol of Li_2O to produce 0.438 mol of B_3^{2-} according to the following reaction:

$$2[BO_{2/2}O]^- + Li_2O = 2[BO_{1/2}O_2]^{2-}$$

All the B_3^- units are exhausted in the process, but the glass composition is so rich in Li_2O that there is still (0.3 − 0.219) = 0.081 mol of it remaining, which can further modify a part of B_3^{2-} to B_3^{3-} by the following reaction:

$$2[BO_{1/2}O_2]^{2-} + Li_2O = 2[BO_3]^{3-}$$

Thus, 0.081 mol of Li_2O use up 0.162 mol of B_3^{2-} to give rise to 0.162 mol of B_3^{3-}. The remaining B_3^{2-} would be (0.438 − 0.162) = 0.276 mol. Modifier Li_2O is thus exhausted. The total of the resulting species in the glass would be 0.162 mol of B_4, 0 mol of B_3^-, 0.276 mol of B_3^{2-}, and 0.162 mol of B_3^{3-}. Expressed in terms of B_2O_3 that has been converted to various B_4 or B_3 species, there is 0.081 mol of B_2O_3 as B_4, 0.138 mol of B_2O_3 as B_3^{2-}, and 0.081 mol of B_2O_3 as B_3^{3-}, which adds up to 0.3 mol of B_2O_3. (These quantities therefore represent the mole fractions of the B_3 and B_4 species as well.) The same procedure has been adopted to calculate the quantities of various B_3 species in other glasses, and they are listed in Table 4. $(\sum B_m^n)/2$ (where $m = 3$, 4 and $n = 1-3$) is equal to the total quantity of B_2O_3 present in the glasses given in Table 1.)

The presence of the various B_3^{n-} species can be expected to exhibit their own spectroscopic features particularly in the Raman spectra. As evident from Table 4, B_3^- is a dominant species in many compositions. B_3^{2-} and B_3^{3-} are present in all glass categories except the CLB series. The concentration of orthoborate species is very low and may not be expected to give rise to strong features in the Raman spectra. However, B_3^{2-} gives rise to absorption features in the region of 800−960 cm^{-1} as seen in the CLOB, CB, and CLSB series. But as noted earlier, these features are not expected to be present in the CLB series,

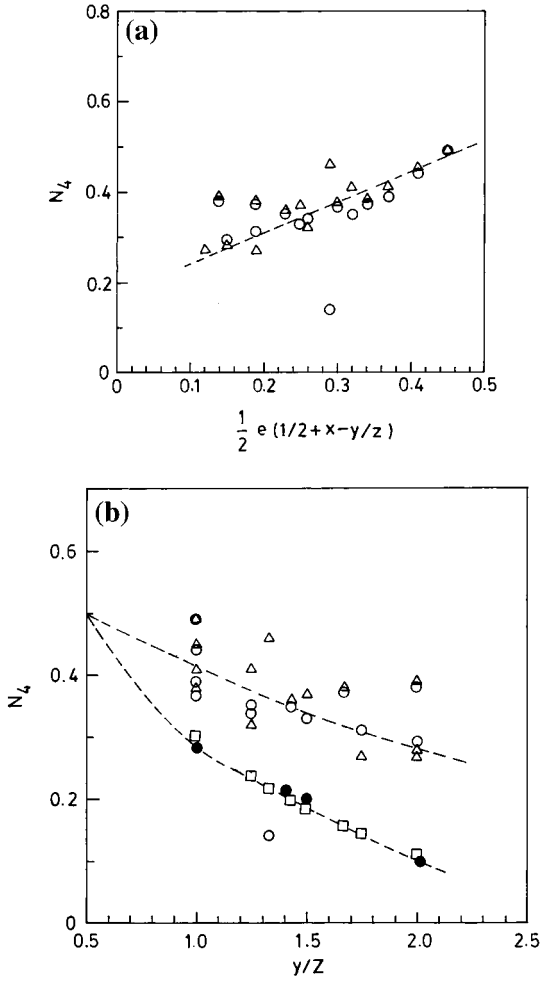

Figure 7. (a) Variation of N_4 determined from NMR and IR plotted as a function of (1/2) exp(1/2 + x − y/z), where x, y, and z are the mole fractions of Li_2SO_4, Li_2O, and B_2O_3, respectively. △ denotes N_4 (NMR), and ○ denotes N_4(IR). (b) Variation of N_4(NMR) (denoted by △), N_4(IR) (denoted by ○), and (1/2) exp(1/2 − y/z) (denoted by □) with y/z. (Experimental points are noted with ● and are taken from ref 45).

but we do observe weak features in this region in Li_2SO_4-rich CLB compositions. This is indicative of some new species arising from sulfate−borate interactions. Spectral features in the region of 800−960 cm^{-1} in other glasses also may be partly due to sulfate−borate interactions.

An important issue in these sulfate−borate glasses is whether sulfate influences the retention of B_4 units and how if B_4 is retained and not allowed to get converted to B_3, then the values of N_4 would be higher than what is expected in the absence of sulfate. Since the ratio of Li_2O to B_2O_3 is greater than 0.5 in all the glasses investigated here (well above the diborate compositions), the N_4 values are expected to be below 0.5 and decrease with increasing Li_2O concentration. N_4 is expected to decrease as a function of y/z, where y and z are the mole fractions of Li_2O and B_2O_3 in the glass compositions. However, if there is an effect of Li_2SO_4 in preventing B_4 from being converted to B_3, N_4 must increase as a function of x in the same region, where x is the mole fraction of Li_2SO_4. Keeping in view that when y/z = 0.5 and x = 0, N_4 would be 0.5, we devise an empirical function F(c) = (1/2) exp(1/2 + x − y/z). Using known values of N_4, x, y, and z, F(c) has been calclated and N_4 has been plotted against F(c) in Figure 7a. It clearly shows a positive correlation between N_4(NMR) and F(c). This confirms that N_4 is dependent on x also and increases as x increases, because increasing y/z in this region (y/z > 1/2) should have caused a decrease of N_4 across the entire compostition range irrespective of y and z.

TABLE 5: Average Electronegativities (χ_a) of the Different Borate Units, Sulfoborate Species, and Sulfate Ion along with the Partial Charges on B, O, and S Atoms (δ_B, δ_O, and δ_S Respectively)

unit	χ_a	δ_B	δ_O	δ_S
$[BO_{3/2}]^0$	2.71	0.39	−0.26	
$[BO_{4/2}]^-$	1.96	0.04	−0.52	
$[BO_{2/2}O]^-$	1.96	0.04	−0.52	
$[BO_{1/2}O_2]^{2-}$	1.4	−0.22	−0.71	
$[BO_3]^{3-}$	0.97	−0.43	−0.86	
$[BO_{3/2}O]^{2-}$	1.4	−0.22	−0.71	
$[SO_4]^{2-}$	2.16		−0.45	−0.19
$[BO_{2/2}OSO_4]^{3-}$	2.08	0.09	−0.48	−0.23
$[BO_{1/2}O_2SO_4]^{4-}$	1.83	−0.02	−0.56	−0.33

Since N_4(NMR) and F(c) are reasonably well correlated, it is worthwhile to examine the correlation between N_4(IR) and F(c). This is done in Figure 7a by plotting (N_4(IR) − 0.15) against F(c). An arbitrary constant of 0.15 is subtracted from N_4(IR) in order to enable superposition of N_4(NMR) and N_4-(IR). It is seen that the two quantities are quite well superposed, suggesting that both NMR and IR are confirming the positive role of SO_4^{2-} in retaining B_4 units in the glass structure.

To further ascertain the effect of lithium sulfate on N_4 in these glasses, N_4(NMR), N_4(IR), and $F(y,z)$ = (1/2) exp(1/2 − y/z) have been together plotted as a function of y/z in Figure 7b. The function $F(y,z)$ is assumed to reflect the variation of N_4 in a sulfate-free modified borate glass in the composition region above y/z = 1/2. Also included in Figure 7b are a few experimental N_4 values observed in Li_2SO_4-free alkali borates.[45] We first note in this figure that the experimental points lie satisfactorily close to those from the empirical function $F(y,z)$. N_4(NMR) and N_4(IR) clearly lie well above the locus of this function confirming the influence of x in retaining N_4.

The influence of Li_2SO_4 upon the retention of B_4 is therefore now established. The origin of this influence requires to be examined further. Spectroscopic techniques (NMR in particular) can only ascertain the presence of B_4 units and not their connectivities. This feature is particularly important in compositions where $\sum B$ (total borate content) is much less than S (total Li_2SO_4) and the borate is present as pyroborate units, which are chain terminators, and orthoborate ions, which are discrete entities. It is therefore reasonable to consider B_4 as a tetrahedral entity whose connection need not be always to other B_n species. We recall that $[BO_{4/2}]^- \leftrightarrow [BO_{2/2}O]^-$ ($B_4 \Leftrightarrow B_3$) equilibrium in the region y/z > 1/2 is driven in the forward direction when oxide ion activity due to the modifier oxide in the system is increased. The species $[BO_{3/2}O]^{2-}$, a B_4 unit with a NBO attached to it, has never been identified in any borate glass. These features suggest that the tetrahedrality of boron is ultimately critically influenced by the electron density around B. The partial charges on the various anionic species B_3^{n-}, B_4, etc. can be calculated approximately by the procedure of Sanderson.[46] These partial charges and the average (group) electronegativities (referred hereafter as simply electronegativities) of the species are listed in Table 5 for the various species relevant for the present situation. The B_4 species, whose concentration has been noted to be higher in the presence of sulfate, may indeed be suspected to originate from reconversion of $[BO_{2/2}O]^-$ by coordination to $[SO_4]^{2-}$, resulting in the formation of sulfoborate units such as $[BO_{2/2}OSO_4]^{3-}$. An examination of Table 5 supports this viewpoint. First of all, we note that when B_3 is converted to B_4 by a bridging oxide ion the partial charge on B decreases from 0.39 to 0.04 but if a B_3

is converted to B_4 by an NBO (resulting species being $[BO_{3/2}O]^{2-}$), the partial charge on B would change to −0.22. But it is experimentally known that this species is unstable and changes to the stable planar pyroborate unit. We consider it as suggestive of a possibility that a tetrahedral borate species is structurally unstable when the partial charge on boron becomes negative. In this light, when a B_3 is converted to B_4 by SO_4^{2-} instead of O^{2-} by coordinating to $[BO_{2/2}O]^-$ forms $[BO_{2/2}OSO_4]^{3-}$, the partial charge on B becomes 0.093, which is even more positive than that in a usual B_4 ($[BO_{4/2}]^-$) unit. Indeed, the partial charge on oxygens (−0.48) is also slightly lower than that in a normal B_4 unit (−0.52). Therefore, boron in a metaborate unit is stabilized as a new B_4 unit when sulfate ions are available for coordination. The electronegativities of B_3^- and SO_4^{2-} units, which are required to react in order to produce the borosulfate units, are 1.96 and 2.16, respectively, whereas that of the $[BO_{2/2}OSO_4]^{3-}$ unit is 2.08, and it lies between the electronegativities of the reactant species. This also confirms that a reaction between metaborate and sulfate units is possible and is asociated with a negative free energy change.[37] A similar reaction between pyroborate and sulfate ions may not be favored because in the resulting species the partial charge on B becomes negative as shown in Table 5. Therefore, pyroborate units may not be coordinated to tetrahedral sulfate units. The preference for metaborate−sulfate reaction is supported by the observation that the 1485 cm^{-1} peak of the metaborate unit weakens on addition of Li_2SO_4 in the Raman spectra (see Figure 5a−d). In some of the compositions where we do not expect the presence of metaborate units and we still see the associated effects, it is possible that the B_3^- unit is produced from B_3^{2-} by a disproportionation of the kind

$$2[BO_{1/2}O_2]^{2-} \leftrightarrow [BO_3]^{3-} + [BO_{2/2}O]^-$$

The resulting $[BO_{2/2}O]^-$ sustains the reaction with sulfate units. However, definitive spectroscopic identification of the formation of the sulfoborate unit has been difficult. Since the B−O−B and S−O−S stretching frequncies are 850 and 730 cm^{-1}, respectively,[27,47] we should expect the B−O−S stretching frequency to be somewhere in the same region of spectra and active in both IR and Raman. Reference was made earlier to the evolution of peaks in the region of 800−950 cm^{-1} in the Raman spectra of the CLB series. In fact, this feature is evident in other glasses also wherever Li_2SO_4 is present. It is therefore tempting to associate the Raman features in this region with B−O−S stretching in borosulfate units, although further work is essential in this regard.

The reaction between B_3^- and SO_4^{2-} can be examined from a thermodynamic point of view. The reaction is represented as $[B_3]^- + [SO_4]^{2-} \rightleftharpoons [B_4SO_4]^{3-}$ with a characteristic equilibrium constant k, where $k = [B_4SO_4]^{3-}/[B_3]^-[SO_4]^{2-}$. We further relate k to ΔG of the reaction as $k = \exp(-\Delta G/RT)$. If we ignore (perhaps not a serious approximation under the circumstances) the influence of ΔS and equate $\Delta G \approx \Delta H \approx \Delta E$ then $k = \exp(-\Delta E/RT)$, where ΔH and ΔE are the enthalpy and energy of the above reaction. This energy can be approximated by using Pauling's relation[48] $\Delta E = 30(\Delta\chi^2)$, where $\Delta\chi$ is the difference between the electronegativities of the reactants B_3^- (1.96) and SO_4^{2-} (2.16). Thus, $\Delta E = 30(0.2)^2$ kcal/mol = 1.2 kcal/mol. If further the equilibrium was frozen at around 600 K, which is the order of T_g of these glasses, then $k = \exp(-(-1200)/(1.987 \times 600)) = 2.7$. Thus, in the case of CLSB1, using eq 1, $[B_4SO_4]^{3-} = 2.7 \times 0.192 \times 0.3 = 0.15$. This is the excess concentration of B_4 arising from sulfate−borate interaction. The excess B_4 is obtained from Figure 7a from N_4(observed) − N_4-(expected) for SO_4^{2-}-free glass. This value is found to be N_4-(excess) × (B_3 + B_4) = 0.15 × 0.35 = 0.05. In view of the approximations in this approach, the agreement between the two B_4(excess) values may be considered as very satisfactory. This further confirms the presence of interaction between SO_4^{2-} and B_3^-.

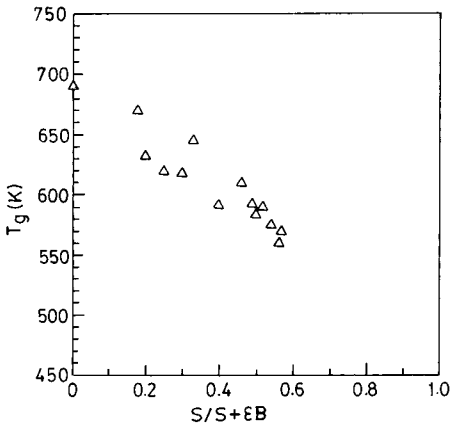

Figure 8. Variation of T_g as a function of the fraction of sulfate ions in the total anion content.

In the presence of such sulfate−borate interactions, it is unlikely that Li_2SO_4 forms microdomains implying a microphase separation. In fact, the borate species listed in Table 4 and the SO_4^{2-} ions (along with the charge compensating Li^+ ions) constitute a homogeneous interacting ion pool whose net effect should manifest in the behavior of glass transition temperatures in these systems. It was seen earlier that T_g decreases with increasing concentration of Li_2SO_4 (see Figure 3). For the reason that T_g was found to vary inversely with the Li_2SO_4 concentration, we have plotted in Figure 8 T_g as a function of the mole fraction of SO_4^{2-} ions ($S/(S + \sum B)$) in the totality of all anionic species present in the system. $\sum B$ represents the sum of all the borate species and S that of SO_4^{2-} ions. It may be seen that there is an essentially linear decrease of T_g. (In passing we may note that extrapolation in Figure 8 gives the T_g of the hypothetical Li_2SO_4 glass as 450 K, identical to what was obtained by similar extrapolation[49] in Li_2SO_4−Li_2O−P_2O_5 glasses). The T_g dependence in Figure 8 indicates a smooth and continuous effect of SO_4^{2-} ions (which evidently weakens the network since T_g decreases) in all the compositions. Therefore, the suggestion of the formation of microdomains of Li_2SO_4 is not supported by the present work.

4. Conclusions

In modified borate glasses, addition of Li_2SO_4 seems to influence the structure of the borate units present. There is evidence from IR, Raman, and ^{11}B MAS NMR spectroscopies of retention of four-coordinate boron in these glasses from an interaction between borate and sulfate units. It has been suggested that sulfoborate species with four-coordinate boron atoms are likely to be formed by the reaction of the sulfate ions with metaborate units. Features in Raman spectra in the region of 800−960 cm^{-1} have been tentatively assigned to the sulfoborate species. Formation of these units manifests as retention of B_4. Variations of glass transition temperatures and molar volumes also seem to support this approach.

Acknowledgment. The authors thank the Commission of the European Communities for financial support. One of the

authors (M.G.) is grateful to the Council for Scientific and Industrial Research (CSIR), India for a senior research fellowship.

References and Notes

(1) Kulkarni, A. R.; Maiti, H. S.; Paul, A. *Bull. Mater. Sci.* **1984**, *6*, 201.
(2) Chowdhari, B. V. R.; Radhakrishna, S. *Materials for solid-state batteries*; World Scientific: Singapore, 1986.
(3) Ingram, M. D. *Phys. Chem. Glasses* **1987**, *28*, 215.
(4) Angell, C. A. *Chem. Rev.* **1990**, *90*, 523.
(5) Angell, C. A. *Annu. Rev. Phys. Chem.* **1992**, *43*, 693.
(6) Rao, K. J.; Ganguli, M. *Handbook of solid-state batteries and capacitors*; World Scientific: Singapore, 1995; p 189.
(7) Levasseur, A.; Cales, B.; Reau, J. M.; Hagenmuller, P. *Mater. Res. Bull.* **1979**, *14*, 921.
(8) Button, D. P.; Tandon, R. P.; Tuller, H. L.; Uhlmann, D. R. *J. Non-Cryst. Solids* **1980**, *42*, 297.
(9) Button, D. P.; Tandon, R. P.; King, C.; Velez, M. H.; Tuller, H. L.; Uhlmann, D. R. *J. Non-Cryst. Solids* **1982**, *49*, 129.
(10) Levasseur, A.; Kabla, M.; Brethous, J. C.; Reau, J. M.; Hagenmuller, P.; Couzi, M. *Solid State Commun.* **1979**, *32*, 839.
(11) Kamitsos, E. I.; Karakassides, M. A.; Chryssikos, G. D. *J. Phys. Chem.* **1986**, *90*, 4528.
(12) Gandhi, P. R.; Deshpande, V. K.; Singh, K. *Solid State Ionics* **1989**, *36*, 97.
(13) Mustarelli, P.; Scotti, S.; Villa, M.; Gandhi, R. *Solid State Ionics* **1990**, *39*, 217.
(14) Chryssikos, G. D.; Kamitsos, E. I.; Patsis, A. P. *J. Non-Cryst. Solids* **1996**, *202*, 222.
(15) Balkanski, M.; Ayyadi, A.; Cadet, P.; Jouanne, M.; Massot, M.; Scagliotti, M.; Levasseur, A. *Solid State Commun.* **1986**, *57*, 41.
(16) Balkanski, M.; Wallis, R. F.; Darianian, I.; Deppe, J. *Mater. Sci. Eng., B* **1988**, *1*, 15.
(17) Balkanski, M.; Darianian, I.; Burret, P. A.; Massot, M.; Julien, C. *Mater. Sci. Eng., B* **1989**, *3*, 177.
(18) Meunier, G.; Dormoy, R.; Levasseur, A. *Mater. Sci. Eng., B* **1989**, *3*, 19.
(19) Julien, C.; Saikh, S. I.; Nazri, G. A. *Mater. Sci. Eng., B* **1992**, *15*, 73.
(20) Cargill, G. S. *Solid-state physics*; Ehrenreich, H., Seitz, F., Eds.; Academic Press: New York; Vol. 30, p 227.
(21) Narsimhan, P. S. L.; Rao, K. J. *J. Non-Cryst. Solids* **1978**, *27*, 225.
(22) Biscoe, J.; Warren, B. E. *J. Am. Ceram. Soc.* **1938**, *21*, 287.
(23) Krogh-Moe, J. *Phys. Chem. Glasses* **1960**, *1*, 26.
(24) Krogh-Moe, J. *Phys. Chem. Glasses* **1962**, *3*, 1, 101, 208.
(25) Krogh-Moe, J. *Phys. Chem. Glasses* **1965**, *6*, 46.
(26) Selvaraj, U.; Rao, K. J. *Spectrochim. Acta* **1984**, *40A*, 1081.
(27) Kamitsos, E. I.; Karakassides, M. A.; Chryssikos, G. D. *Phys. Chem. Glasses* **1987**, *28*, 203.
(28) Kamitsos, E. I.; Karakassides, M. A.; Chryssikos, G. D. *J. Phys. Chem.* **1987**, *91*, 1073.
(29) Kamitsos, E. I.; Patsis, A. P.; Karakassides, M. A.; Chryssikos, G. D. *J. Non-Cryst. Solids* **1990**, *126*, 52.
(30) Konijnendijk, W. L.; Stevels, J. M. *J. Non-Cryst. Solids* **1975**, *18*, 307.
(31) Kamitsos, E. I.; Karakassides, M. A. *Phys. Chem. Glasses* **1989**, *30*, 19.
(32) Kamitsos, E. I.; Karakassides, M. A.; Patsis, A. P. *J. Non-Cryst. Solids* **1989**, *111*, 252.
(33) Chryssikos, G. D.; Kamitsos, E. I.; Patsis, A. P.; Karakassides, M. A. *Mater. Sci. Eng. B* **1990**, *7*, 1.
(34) Meera, B. N.; Ramakrishna, J. *J. Non-Cryst. Solids* **1993**, *159*, 1.
(35) Dillon, K. B.; Waddington, T. C. *Spectrochim. Acta* **1974**, *30A*, 1873.
(36) Prabakar, S.; Rao, K. J.; Rao, C. N. R. *Proc. Royal Soc. (London) A* **1990**, *429*, 1.
(37) Muthupari, S.; Rao, K. J. *J. Phys. Chem.* **1994**, *98*, 2646.
(38) Silver, A. H.; Bray, P. J. *J. Chem. Phys.* **1958**, *19*, 984.
(39) Bray, P. J.; O'Keefe, J. G. *Phys. Chem. Glasses* **1963**, *4*, 37.
(40) Greenblatt, S.; Bray, P. J. *Phys. Chem. Glasses* **1967**, *8*, 213.
(41) Jellison, G. E., Jr.; Bray, P. J. *J. Non-Cryst. Solids* **1978**, *29*, 187.
(42) Fyfe, C. A. *Solid State NMR for chemists*; CNC Press: Guleph, 1983.
(43) Bray, P. J. *J. Non-Cryst. Solids* **1985**, *75*, 29.
(44) Yun, Y. H.; Bray, P. J. *J. Non-Cryst. Solids* **1981**, *44*, 227.
(45) Zhong, J.; Bray, P. J. *J. Non-Cryst. Solids* **1989**, *111*, 67.
(46) Sanderson, R. T. *Polar Covalence*; Academic Press: New York, 1983.
(47) Brown, R. G.; Ross, S. D. *Spectrochim. Acta* **1972**, *28A*, 1263.
(48) Pauling, L. *The nature of chemical bond*; Cornell University Press: Ithaca, NY, 1960; p 64.
(49) Ganguli, M.; Rao, K. J. Personal comunication.